HHS Public Access

Author manuscript

Nat Struct Mol Biol. Author manuscript; available in PMC 2011 June 01.

Published in final edited form as:

Nat Struct Mol Biol. 2010 December ; 17(12): 1453–1460. doi:10.1038/nsmb.1937.

Initiation complex dynamics direct the transitions between distinct phases of early HIV reverse transcription

Shixin Liu[1,6], **Bryan T. Harada**[2,6], **Jennifer T. Miller**[3], **Stuart F. J. Le Grice**[3], and **Xiaowei Zhuang**[1,4,5]

[1] Department of Chemistry and Chemical Biology, Harvard University, Cambridge, Massachusetts, USA

[2] Graduate Program in Biophysics, Harvard University, Cambridge, Massachusetts, USA

[3] HIV Drug Resistance Program, National Cancer Institute, Frederick, Maryland, USA

[4] Department of Physics, Harvard University, Cambridge, Massachusetts, USA

[5] Howard Hughes Medical Institute, Harvard University, Cambridge, Massachusetts, USA

Abstract

Human immunodeficiency virus (HIV) initiates reverse transcription of its viral RNA (vRNA) genome from a cellular $tRNA^{Lys,3}$ primer. This process is characterized by a slow initiation phase with specific pauses, followed by a fast elongation phase. We report a single-molecule study that monitors the dynamics of individual initiation complexes, comprised of vRNA, tRNA and HIV reverse transcriptase (RT). RT transitions between two opposite binding orientations on tRNA:vRNA complexes, and the prominent pausing events are caused by RT binding in an flipped orientation opposite to the polymerization-competent configuration. A stem-loop structure within the vRNA is responsible for maintaining the enzyme predominantly in this flipped orientation. Disruption of the stem-loop structure triggers the initiation-to-elongation transition. These results highlight the important role played by the structural dynamics of the initiation complex in directing transitions between early reverse transcription phases.

As a key step in the life cycle of HIV, reverse transcription converts the single-stranded vRNA genome into an integration-competent double-stranded DNA[1]. This multi-step reaction is catalyzed by the viral enzyme RT, which initiates DNA synthesis from the 3′ terminus of a cell-derived $tRNA^{Lys,3}$ annealed to an 18-nucleotide (nt) primer binding site (PBS) in the vRNA[2]. As a prerequisite of reverse transcription, the tRNA primer, vRNA template and RT must assemble into a productive ternary ribonucleoprotein complex, called the initiation complex[3–5]. Various chemical and enzymatic probing assays have revealed

Correspondence should be addressed to X.Z. (zhuang@chemistry.harvard.edu).

[6]These authors contributed equally to this work.

AUTHOR CONTRIBUTIONS

S.L., B.T.H. and X.Z. designed the experiments; S.L. and B.T.H. performed the experiments and analyzed the data; S.L., B.T.H., and X.Z. interpret the data and wrote the paper; J.T.M. made the enzyme and some of the tRNA constructs; S.F.Le G. contributed to discussion, data interpretation and manuscript preparation.

extensive intermolecular interactions within this complex, which are important for the efficiency and specificity of the initiation of minus-strand DNA synthesis[6–10].

The early stages of reverse transcription comprise a slow, distributive initiation phase followed by a fast, processive elongation phase[11,12]. The initiation phase is characterized by slow DNA polymerization, rapid dissociation of RT, and frequent kinetic pauses during primer extension. These pausing events result in the accumulation of short extension products, such as the tRNA+3 and tRNA+5 intermediates. Interestingly, after addition of the 6th nucleotide to the tRNA primer, reverse transcription transitions to the elongation phase with dramatically increased polymerization rate and processivity[13]. The unique and complex nature of the initiation process makes it an attractive target for antiviral drugs. Indeed, it has been shown that some RT inhibitors and drug-resistant RT mutants have different effects on initiation versus elongation[9]. Elucidating the mechanism underlying the initiation process could therefore set the stage for developing novel inhibitors for combating HIV infection. However, a consensus on the structure of the initiation complex has yet to be reached[7,14,15]. Furthermore, the dynamics of the complex and the mechanism underlying the transitions between various phases of early reverse transcription remain incompletely understood[13,16–19].

We recently demonstrated that RT displays remarkable orientational and translational dynamics on its nucleic acid substrates[20,21]. Such large-scale motions facilitate various stages of reverse transcription, including DNA synthesis, RNase H cleavage, and strand-displacement synthesis. In particular, RT can bind its substrates in two opposite orientations[20,22]. In one orientation, the DNA polymerase active site is positioned over the 3′ end of the primer, ready to catalyze primer extension. In the other, RT is flipped ~180 degrees such that the DNA polymerase active site is physically separated from the primer 3′ end, and thereby unable to support synthesis. Here, we investigated whether such orientational dynamics regulate the initiation of reverse transcription.

To test this hypothesis, we applied single-molecule fluorescence resonance energy transfer (FRET)[23,24] and ensemble primer-extension assays to probe the conformation and enzymatic activity of the initiation complex. Interestingly, we found that this complex supports both the polymerase-competent and the flipped RT binding orientations. Furthermore, the equilibrium between these two binding orientations evolves as RT elongates the tRNA primer, and changes in the primer extension activity correlate with changes in the enzyme's binding orientation. In particular, a stem-loop structure within the vRNA adjacent to the PBS forces RT to bind predominantly in the flipped, polymerization-incompetent orientation, causing reverse transcription pauses. Disrupting this structure by strand-displacement synthesis allows RT to bind in the polymerase-competent mode and triggers the initiation-to-elongation transition.

RESULTS

Single-molecule assay for studying initiation complex dynamics

To facilitate single-molecule FRET measurements, we labeled specific sites of the initiation complex with FRET donor and acceptor dyes. First, we constructed a vRNA template using

the sequence corresponding to nucleotides 106–245 of the HIV-1 genome (NL4.3 isolate), with the PBS located at nucleotides 183–200. It has been shown that the sequence within the initiation site of the NL4.3 isolate is representative of 86% known HIV-1 isolates[14] and that sequences outside this region do not affect the efficiency of reverse transcription[25]. A FRET acceptor dye (Cy5) was site-specifically attached to U208 near the 3′ end of the PBS (Fig. 1a). The natural $tRNA^{Lys,3}$ primer was then annealed to the PBS. Next, tRNA:vRNA complexes were anchored to a slide surface and immersed in a reaction buffer containing HIV-1 RT labeled with a FRET donor dye (Cy3) at its RNase H domain (Fig. 1a). Dye labeling of RT and vRNA did not alter reverse transcription kinetics appreciably (Supplementary Fig. 1). Fluorescence emission from individual tRNA:vRNA:RT ternary complexes was monitored using a total-internal-reflection fluorescence microscope. Freely diffusing RT was observed to bind and dissociate from the tRNA:vRNA substrates in real time. Each binding event caused an increase in the total fluorescence signal due to excitation of the FRET donor dye (Fig. 1b). FRET values recorded during the binding event allowed us to determine the binding configuration of the enzyme. In this scheme, dissociation of the enzyme would result in a loss of the total fluorescence signal while a FRET value change without loss of total fluorescence could be interpreted as a change of binding configuration. In addition to the tRNA:vRNA substrates, we also probed the binding configuration of RT on substrates comprising a variety of primer and template structures, as shown in Fig. 1c,d.

RT adopts two opposite orientations in initiation complexes

It has been shown that HIV-1 RT can bind to simple primer:template substrates in two opposite orientations[20],[22]: In the case of a DNA primer, RT binds almost exclusively in the polymerase-competent orientation; in the case of a random-sequence RNA primer annealed to a simple DNA template, RT binds in the flipped orientation that inhibits primer extension. It is thus interesting to ask which orientation RT would adopt on the substrate formed between two complex RNA structures (tRNA and vRNA), which supports primer extension despite its RNA primer composition. Should RT bind in the polymerase-competent orientation, we expect to observe a high FRET value due to the proximity of the FRET donor and acceptor dyes according to previous crystallographic and footprinting data[26–28]. In contrast, the flipped orientation should give a low FRET value of ~0.2–0.3 with the donor and acceptor separated by the 18-base-pair tRNA:PBS duplex (Fig. 2a).

Notably, the binding of RT to the tRNA:vRNA complex gave two distinct FRET peaks centered at ~0.9 and ~0.2 (Fig. 2b), suggesting that RT binds in both the polymerase-competent and flipped orientations on this substrate. To confirm the assignments of the two FRET states, we took advantage of the knowledge that cognate deoxyribonucleotides preferentially stabilize RT binding in the polymerase-competent orientation[20]. Indeed, when the FRET distribution was acquired in the presence of the cognate nucleotide (over a short duration to avoid substantial primer extension), the equilibrium shifted towards the high FRET state (Fig. 2b), supporting the assignment of this state to the polymerase-competent binding mode. The two binding modes were also observed when the $tRNA^{Lys,3}$ primer was annealed to a simple RNA template containing the PBS sequence without any secondary structures (Fig. 1c and Supplementary Fig. 2), further supporting the notion that the two FRET states originate from different binding configurations of RT on the tRNA:PBS duplex

rather than binding to regions of vRNA outside the PBS. Moreover, the FRET time trace showed spontaneous transitions between the ~0.9 and ~0.2 FRET states within individual binding events (Fig. 2c), indicating that RT could dynamically transition between the two orientations without dissociation.

We next studied the influence of tRNA structure on RT binding orientation by testing substrates formed by various other primers (Fig. 1d) and the vRNA template. First, we replaced the natural $tRNA^{Lys,3}$ with a synthetic, unmodified tRNA (syn-tRNA) to test the effect of the modified tRNA bases. The FRET distribution observed for the syn-tRNA:vRNA:RT complexes was similar to that of $tRNA^{Lys,3}$:vRNA:RT (Supplementary Fig. 3a,b). The equilibrium constant (*K*) between the high-FRET and low-FRET orientations was 0.54 ± 0.06 for natural $tRNA^{Lys,3}$ and 0.64 ± 0.10 for syn-tRNA, respectively. Next, an 18-nt oligoribonucleotide (ORN) primer complementary to the PBS was used in place of $tRNA^{Lys,3}$. In this case, RT can still transition between the two orientations, the equilibrium shifting towards the high-FRET orientation with $K = 1.8 \pm 0.2$ (Supplementary Fig. 3c). It has been suggested that the anti-codon loop of the tRNA base-pairs with the A-rich loop upstream of the PBS, although results on whether such interactions exist in the NL4.3 isolate vary[14,15,29]. Since such interactions would not be present in the case of the ORN primer, our results indicate that the ability of RT to adopt and flip between the two orientations does not require these interactions outside the PBS. Finally, when an 18-nt oligodeoxyribonucleotide (ODN) primer was annealed to the vRNA template, RT nearly exclusively bound in the high-FRET, polymerase-competent orientation (Supplementary Fig. 3d). In addition, the average binding time of RT was substantially longer on the ODN primer (40 sec) than on the ORN (2.0 sec) and tRNA (1.6 sec) primers. These results indicate that both the nucleotide nature (deoxyribonucleotide vs. ribonucleotide) and the secondary structure of the primer play a role in determining RT's binding orientation.

Polymerase activity correlates with RT binding orientation

To investigate how RT's binding orientation changes during the initiation of minus-strand DNA synthesis, we constructed a series of tRNA-DNA chimeras, tRNA+*n*, representing intermediates encountered at varying primer extension steps (*n* denotes the number of deoxyribonucleotides added to the tRNA 3′ terminus) (Supplementary Fig. 4). Cy3-labeled RT was then added to the Cy5-labeled tRNA+*n*:vRNA substrates. All tRNA+*n*:vRNA:RT initiation complexes ($n = 0 – 6$) supported both high and low FRET binding orientations (Fig. 2b and Supplementary Fig. 5a). The equilibrium constant *K* between the two FRET states increased when *n* increased from 0 to 2 (Fig. 2b,d**and** Supplementary Fig. 5). Remarkably, when tRNA was further extended by one extra nucleotide (i.e. tRNA+3), RT binding shifted substantially towards the flipped orientation, which remained dominant until position tRNA+5 (Fig. 2b,d **and** Supplementary Fig. 5). Finally, when the 6^{th} nucleotide was added to the tRNA primer, another major shift occurred, resulting in a predominant polymerase-competent binding orientation for the enzyme (Fig. 2b,d **and** Supplementary Fig. 5). Analysis of the flipping rate constants indicates that the change in the flipping equilibrium is modulated primarily by the rate at which RT transitions from the polymerase-competent to the flipped orientation whereas the reverse rate does not vary substantially with the length of the DNA extension (Supplementary Fig. 5b).

Intriguingly, the positions at which the binding orientation equilibrium undergoes major changes (tRNA+3 and tRNA+6) correspond to major transitions in primer extension kinetics: polymerization exhibits a strong pause at tRNA+3 and a transition from the slow initiation phase to the rapid elongation phase at tRNA+6(Refs.[11],[13]). These correlations raise the possibility that the DNA synthesis activity of RT during initiation may be regulated by its binding orientation. To test this notion, we performed single-turnover nucleotide incorporation assays to determine the primer extension activity of RT on all reaction intermediates used in the single-molecule FRET experiments. Indeed, the primer-extension rate was closely correlated with the equilibrium between the two binding orientations (Fig. 2d,e). In particular, RT exhibited the lowest primer extension activity on the tRNA+3 primer, where the enzyme preferentially bound in the flipped orientation, and the fastest extension kinetics on tRNA+6, where the enzyme predominantly bound in the polymerase-competent orientation. These observations suggest that the polymerase activity of the enzyme is at least in part regulated by its binding orientation.

Stem-loop near PBS causes reverse transcription pausing

Next we investigated the origin of the pauses during early reverse transcription, namely the structural features of the initiation complex responsible for the flipped RT binding orientation and slow primer extension rate. The most prominent pause during initiation is at position +3, for which two possible scenarios may be hypothesized: (i) the 3-nt DNA addition to the tRNA primer may confer on it a unique structure (or primer:PBS duplex structure) that disfavors RT binding in the polymerase-competent orientation; (ii) alternatively, the stem-loop structure in the vRNA template 3-nt upstream of the PBS[14],[16] may force RT to bind in the flipped orientation and decrease DNA synthesis activity. To distinguish between these possibilities, we compared the binding configuration and primer extension kinetics of RT on the simple PBS template (Fig. 1c) to those on the vRNA template. While RT preferentially bound in the low FRET state on the tRNA+3:vRNA substrate, it strongly favored the high FRET, polymerase-competent orientation on the tRNA +3:PBS substrate (Fig. 3a). Moreover, the substantial drop of primer extension rate from the tRNA+2 to tRNA+3 position observed on the vRNA template was not reproduced on the simple PBS template (Fig. 3a). As a result, unlike in the case of the vRNA template, no substantial pause was detected at position +3 on the simple PBS template (Supplementary Fig. 6a, b). These results indicate that the strong +3 pause on the vRNA template is not due to an intrinsic structural property of the tRNA+3 primer, but rather originates from the template structure.

To test the role of the vRNA stem-loop structure in regulating RT's binding dynamics, we created a mutant, $vRNA_{h-}$, by altering the sequence at positions 135–142 such that the 8 base pairs at the base of the stem-loop could not form (Fig. 3b). When RT was added to the tRNA+3:$vRNA_{h-}$ substrate, the FRET distribution showed a single peak at ~0.9 (Fig. 3b), indicating binding predominantly in the polymerase-competent orientation. This result differs drastically from the behavior of RT on the wild type vRNA template but mimics its interaction with the simple PBS template. Moreover, the single-nucleotide incorporation assay showed that eliminating the stem-loop structure in the $vRNA_{h-}$ template increased the primer extension rate at the +3 position by ~8 fold compared to the wild type vRNA (Fig.

3b), consistent with a previous report that altering vRNA sequences upstream of the PBS can eliminate the +3 pause site[16]. Overall, the above observations demonstrate that the secondary structure of the vRNA template strongly influences the binding configuration of RT: the stem-loop structure upstream of the PBS reorients RT into a flipped, polymerase-incompetent orientation and induces pausing at position +3.

Conflicting results have been reported on whether the same +3 pause occurs when a DNA primer is used[11],[16]. Interestingly, we found that the ability of the stem-loop to reorient RT vanished when the tRNA was replaced by an ODN primer. RT bound predominantly in the polymerization orientation on an ODN+3:vRNA substrate despite the presence of the stem-loop structure (Supplementary Fig. 6c). Furthermore, RT exhibited much weaker pausing at the +3 position when reverse transcription was initiated from the ODN primer (Supplementary Fig. 6d). This observation rules out the possibility that the strong +3 pause observed with the tRNA primer is due to the intrinsically slower rate of strand-displacement synthesis[30] as the enzyme passes through the vRNA stem-loop, which should occur for both tRNA and ODN primers, and further supports the notion that the flipped RT orientation on the tRNA:vRNA substrate imposed by the stem-loop was a major determinant of pausing.

Disruption of stem-loop triggers transition to elongation

Because the stem-loop structure induces strong pausing and consequently the slow, distributive initiation phase of DNA synthesis, we hypothesize that disassembly of the stem-loop structure may cause the transition to the elongation phase that occurs between tRNA+5 and tRNA+6. Supporting this hypothesis, such a transition was not observed on the simple PBS template lacking the stem-loop structure, on which the tRNA+6 and tRNA+5 primers displayed similar extension kinetics (Fig. 3a).

If unfolding of the stem-loop structure mediates the initiation-to-elongation transition, we anticipate that preventing hairpin disassembly would inhibit entry into the elongation phase. We therefore created another mutant vRNA template containing a hairpin structure lacking bulges ($vRNA_{h+}$), which should be more stable and difficult to disrupt. Indeed, this modification shifted the binding configuration of RT toward the low FRET orientation (Fig. 3c). In addition, the tRNA+6:$vRNA_{h+}$ substrate displayed a primer extension rate that was substantially slower as compared to the wild type tRNA+6:vRNA case but was more similar to those of the initiation phase (Fig. 3c). These results suggest that entry into the elongation phase requires disassembly of the stem-loop structure.

To further test this notion, we directly probed the stem-loop structure by placing Cy3 and Cy5 on U132 and U177 of the vRNA, respectively (Fig. 4a). A fully formed hairpin would bring the two dyes into proximity and generate a high FRET value, whereas an opened hairpin would force them apart and yield a low FRET value. The doubly-labeled vRNA template was then annealed to various tRNA+*n* primers and incubated with unlabeled RT. In the case of an unextended tRNA primer, a major FRET peak at 0.95 was observed (Fig. 4b), reflecting a folded stem-loop structure. Similar FRET distributions were observed for the tRNA+3:vRNA and tRNA+5:vRNA substrates (Fig. 4c,d), indicating that the stem-loop was still largely intact after incorporation of up to five deoxyribonucleotides. In contrast, in the presence of tRNA+6, the majority of complexes exhibited a low FRET value ~0.15 (Fig.

4e), indicating opening of the hairpin structure. Presumably, in the tRNA+6:vRNA:RT complex, competition from the terminal three nucleotides of tRNA+6 destabilizes the stem-loop and, together with the bulges in the upper half of the stem-loop, makes this structure relatively unstable. Unfolding of the stem-loop structure explains why RT can engage this substrate predominantly in the polymerase-competent mode (Fig. 2b,d) and synthesize DNA efficiently (Fig. 2e).

Role of NC in the initiation phase of DNA synthesis

The viral nucleocapsid (NC) protein has been reported to facilitate various stages of HIV replication, including reverse transcription[31,32]. NC is a small basic protein that nonspecifically binds to nucleic acids and possesses nucleic-acid chaperon activity[32,33]. In particular, it has been suggested that NC could disrupt template secondary structures at which RT pauses during the elongation phase[34–36]. It is thus interesting to ask whether NC could disrupt the stem-loop structure upstream of the PBS and increase the primer extension rate at the +3 position. Addition of NC to the doubly-labeled tRNA:vRNA complex broadened the FRET distribution considerably (Fig. 5a). FRET traces of individual initiation complexes revealed fluctuations among a wide range of FRET values (Fig. 5a), suggesting NC-mediated destabilization of the stem-loop. A recent high-throughput footprinting study also shows that the stem-loop upstream of the PBS is at least partially open in the virus particle while disruption of the NC-vRNA interactions restores base-pairing[15]. With the stem-loop structure disrupted, we anticipate that RT would bind primarily in the polymerase-competent orientation. Indeed, when added to the Cy5-labeled tRNA+3:vRNA substrate in the presence of NC, Cy3-labeled RT bound predominantly in the high FRET, polymerase-competent orientation, in contrast to the case without NC (compare Fig. 5b with the tRNA+3 panel in Fig. 2b). Intriguingly, despite the disruption of the stem-loop, the addition of NC did not result in appreciable increase in the extension rate of the tRNA+3 primer (Fig. 5c), consistent with previous observations[16,19]. Considering that NC binding may reduce binding of RT to the primer:template complex[36] and inhibit DNA synthesis due to steric hindrance[37], these negative effects could counter-balance its effect on disrupting the stem-loop structure. Indeed, we observed a substantial reduction in the binding frequency of RT to the tRNA+3:vRNA substrate in the presence of NC in single-molecule FRET traces (not shown), and NC has been previously found to have both positive and negative effects on reverse transcription depending on the experimental conditions[34–38]. It is worth noting that NC is present at an extremely high concentration in the virions and such a condition is difficult to simulate *in vitro* due to protein aggregation. Future experiments that probe the virus directly are required to further elucidate whether the initiation pauses are alleviated by NC.

DISCUSSION

Reverse transcription of the HIV genome is initiated from a cellular tRNA primer bound to the viral RNA. The specific structure and dynamics of the tRNA:vRNA complex result in an initiation phase with properties markedly different from those of later stages of reverse transcription, providing unique opportunities for anti-HIV drug design. It is thus important

to understand the correlation between the structural dynamics of the initiation complex and their functional consequences.

By monitoring the dynamics of individual initiation complexes in real time, we investigated in detail how HIV-1 RT interacts with tRNA:vRNA substrates. Our results reveal that RT adopts two orientations in the initiation complex — a polymerase-competent orientation and a flipped orientation in which the polymerase active site is placed many nucleotides from the 3′ end of the tRNA, precluding primer extension. The equilibrium between these two orientations regulates RT activity throughout the initiation process (Fig. 6). The relatively slow polymerization rates during initiation result in part from the fact that RT spends a large portion of time bound to the tRNA:vRNA substrate in the flipped, polymerase-incompetent orientation (Fig. 6), though the nucleotide nature of the primer (RNA vs. DNA) and the secondary structure of the template, which determines whether RT has to undergo strand-displacement synthesis, could also affect polymerization kinetics directly[13],[16],[17]. Interestingly, the ability to support RT binding in the flipped, polymerase-inactive orientation is a unique property of the RNA primer. When the tRNA primer is replaced with a DNA primer complementary to the PBS sequence, RT binds to the primer:template complex nearly exclusively in the polymerase-competent orientation and a slow initiation phase is not observed (Supplementary Fig. 6).

Addition of the first few nucleotides to the tRNA primer leads to a shift of the RT binding equilibrium towards the polymerase-competent orientation and an increase in the DNA synthesis rate (Fig. 6). This rate then drops dramatically at position +3, where RT encounters a stem-loop structure on the vRNA template that forces the enzyme to bind predominantly in the flipped, polymerase-inactive orientation, increasing the probability of pausing (Fig. 6). RT cannot escape this slow mode of synthesis until it has synthesized enough DNA to disrupt the stem-loop at position +6. Disassembly of the stem-loop allows RT to reorient into the polymerase-competent binding mode and triggers transition to the fast, processive elongation phase of DNA synthesis (Fig. 6). The single-stranded bulges within the vRNA stem-loop appear to promote the initiation-to-elongation transition (Fig. 3c). Taken together, the above results provide a structural basis for understanding the early stages of reverse transcription and demonstrate how the structural dynamics of the initiation ribonucleoprotein complex regulate RT activity.

Considering the critical role played by the stem-loop in regulating RT binding orientation and activity, it is interesting to speculate that HIV may have evolved this structure to act as a temporal brake to slow initiation of reverse transcription. Such a mechanism may help prevent reverse transcription of the RNA genome prior to virus budding[39],[40], which is detrimental to viral infectivity[31],[41]. This speculation is supported by the observations that both mutations of the viral NC protein that cause premature reverse transcription and mutations near the vRNA PBS that increase the initiation efficiency result in virus replication defects[42–44]. Conveniently, the NC protein has an ability to unwind the stem-loop (Fig. 5a) and evidence suggests that this stem-loop is partially disrupted within the virus particle[15]. Therefore, this mechanism to inhibit reverse transcription in the initiation phase may be partially alleviated in a matured virion. On the other hand, the precursor form of NC within the Gag polyprotein (the form found in infected cells prior to virus budding)

appears to have a weaker chaperone activity than the cleaved form of NC present in mature virions[45], potentially making the inhibition mechanism stronger prior to virus budding to prevent premature reverse transcription. Although it is difficult to mimic the exact effects of NC *in vitro*, future *in virio* and *in vivo* experiments should help test these hypotheses.

These unique properties of the initiation complex could make it an attractive target for the development of anti-HIV agents[9]. Indeed, initiation can be suppressed by both nucleoside-analog and non-nucleoside RT inhibitors, some of which display higher efficacy during initiation than elongation[46],[47]. The structural and mechanistic understanding of the initiation process demonstrated here could potentially help the development of novel antiviral agents, in particular by designing drugs that regulate the structural dynamics of the viral RNA and the binding orientation of RT, two factors of critical importance during early reverse transcription.

METHODS

Protein preparation

Recombinant HIV-1 RT p66 and p51 subunits were expressed and purified as described previously[48]. An E478Q mutation was introduced into the p66 RNase H domain to eliminate RNase H activity and prevent degradation of the substrates[49]. To produce Cy3-labeled RT, the native cysteines on RT were changed to serine and a unique cysteine residue was introduced at the C-terminus of the p66 subunit. Purified RT molecules were incubated with Cy3 maleimide (GE Healthcare) for 60 minutes in 100 mM pH 7.0 NaH_2PO_4/Na_2HPO_4 buffer. Labeled RT was then dialyzed for ~ 48 hours to remove excess dye molecules. NC protein was a gift from Dr. Robert Gorelick (National Cancer Institute, Frederick, MD).

Nucleic acid preparation

Natural $tRNA^{Lys,3}$ purified from human placenta was purchased from Bio S&T. Natural tRNA-DNA chimeras were generated by employing RNaseH cleavage[50] followed by a splinted ligation as shown in Supplementary Fig. 4. Synthetic DNA (Integrated DNA Technologies) and RNA (Dharmacon) oligonucleotides were purified by denaturing polyacrylamide gel electrophoresis. vRNA templates longer than 80 nt were constructed by ligating two synthetic RNA pieces with T4 RNA ligase 2 (New England Biolabs). When necessary, the strands were specifically derivatized with a biotin or an amino modifier during synthesis. Cy3 or Cy5 mono-reactive NHS ester (GE Healthcare) was post-synthetically conjugated to the primary amine group on DNA or RNA. Labeled oligonucleotides were HPLC purified by reverse phase chromatography on a C8 column (GE Healthcare). To assemble a primer:template complex, primer and template strands were annealed with a 10:1 ratio in the annealing buffer (50 mM pH 8.0 Tris-HCl, 100 mM KCl, and 1 mM EDTA) using a Bio-Rad thermocycler with the following program: 2 minute at 95 °C followed by 10 minutes at 70 °C, then slowly cool down to 4 °C over 1 hour. Annealed products were analyzed on 5% native polyacrylamide gels to confirm successful assembly. Excess, unannealed primer molecules do not affect analysis as they are neither labeled by dye for detection nor labeled by biotin to allow surface anchoring.

Single-molecule FRET measurement

Nucleic acid substrates were immobilized on PEG-coated quartz microscope slides through biotin-streptavidin linkage as previously described[20]. The biotin group was placed at the 5′ end of the template strand in all constructs. Surface-immobilized Cy5-labeled substrates were immersed in a solution containing Cy3-labeled RT. Measurements were performed in standard RT reaction buffer (50 mM pH 8.0 Tris-HCl, 50 mM KCl, 6 mM $MgCl_2$, and 0.1 mg ml^{-1} BSA) at room temperature (23 °C). An oxygen scavenger system (10% w/v glucose, 300 μg ml^{-1} glucose oxidase, and 40 μg ml^{-1} catalase) and a reducing reagent (2 mM Trolox)[51] were included in the buffer to minimize photobleaching and blinking. The concentration of Cy3-labeled p66 subunits used in the single-molecule experiments was 10 – 20 nM. A large excess of unlabeled wildtype p51 subunits, at a concentration (100 – 200 nM) comparable to or larger than the dissociation constant of the p66/p51 heterodimer[52] were added such that a substantial fraction of the Cy3-labeled p66 form heterodimers with p51. As the p66 and p51 subunits alone exhibited much lower affinities to the nucleic acid substrates and the p66 subunits were present at a much lower concentration than the dissociation constant of the p66/p66 homodimer[52], the majority of the binding events that we observed should involve a p66/p51 heterodimer. The observation of single-step RT dissociation or Cy3 photobleaching indicates that the observed binding events were from a single RT molecule.

The fluorescence signals for the FRET donor Cy3 and acceptor Cy5 were detected using a prism-type total-internal-reflection fluorescence microscope[20]. Alternating 532 nm (Crystal Laser) and 635 nm (Coherent) laser light were used to excite the sample[53]. Emission from the donor and acceptor were separated using a dichroic mirror (Chroma Technology) and imaged onto the two halves of a back-illuminated electron multiplying CCD camera (Andor Ixon 887). The FRET value during RT binding events was defined as $I_A/(I_A + I_D)$, where I_A and I_D were the fluorescence signals detected from the acceptor and donor channel, respectively.

To accurately identify RT binding events to nucleic-acid substrates, RT molecules nonspecifically adhered to the slide surface need to be excluded as these molecules give a donor-only signal that could be mistaken as substrate-specific binding events with FRET = 0. Here, in addition to using PEG-coated slides to minimize nonspecific sticking of RT to the surface, we further developed an algorithm to identify the remaining nonspecific surface-binding events using high-precision single-molecule localization, which allowed us to exclude these events during data analysis. In this assay, images of individual RT and substrate molecules, taken during 532 nm and 635 nm illumination, respectively, were fit to a Gaussian function to locate their centroid positions. A RT molecule within 0.5 pixels (~70 nm) of a substrate molecule was considered bound specifically to the substrate (Supplementary Fig. 7). While the image of a single molecule is diffraction limited (image width ~ a few hundred nanometers), the position of the molecule can be determined to a much higher precision depending on the number of photons detected[54,55]. Thus, this single-molecule localization assay allows us to determine specific binding events with much higher fidelity than simply identifying overlapping Cy3 and Cy5 images.

Single-turnover nucleotide incorporation kinetics assay

The primer:template substrates were annealed as described above. Cy5 (GE Healthcare) was conjugated to the primers at the 5′ end (ODN and ORN primers) or at position U67 (tRNA primers) to monitor DNA synthesis. Substrates (5 nM) were incubated with a saturating concentration of RT (~500 nM) in RT reaction buffer at room temperature for 5 minutes in a final reaction volume of 100 μl. Single nucleotide incorporation was initiated by the addition of selected dNTP (200 μM final concentration) and terminated by mixing a 5 μl aliquot of the reaction mixture with 15 μl of stop buffer (96% v/v formamide, 20 mM EDTA) at various time points. Reaction products were heated to 95 °C for 5 minutes, fractionated over a 6% (tRNA primers) or 10% (ODN and ORN primers) denaturing polyacrylamide gel, and quantified using a Typhoon Trio Imager (GE Healthcare).

RT pausing assays

The reactions were prepared as above with the following changes. To better detect the faint intermediate bands, primers were radiolabeled with ^{32}P using the KinaseMax kit (Ambion). Subsaturating concentrations of RT were used (20 nM for ODN, 50 nM for tRNA). Reactions were initiated by the addition of all four dNTPs (200 μM final concentrations) and terminated by mixing a 5 μl aliquot with 15 μl of stop buffer. Reaction products were fractionated over a denaturing polyacrylamide gel as above, exposed onto a PhosphoImager cassette (GE Healthcare), and quantified using the Typhoon Trio Imager.

Supplementary Material

Refer to Web version on PubMed Central for supplementary material.

Acknowledgments

We thank John Wu and Elio Abbondanzieri for helpful discussions, and Robert Gorelick (National Cancer Institute, Frederick, MD) for providing NC proteins. This work is supported in part by NIH (GM 068518 to X.Z.) and the Intramural Research Program of the Center for Cancer Research, NCI (to S.F.J.L.G.). B.T.H was supported by a NIH/NIGMS Molecular Biophysics Training Grant (GM008313 to the Harvard Biophysics Program). X.Z. is a Howard Hughes Medical Institute investigator.

References

1. Telesnitsky, A.; Goff, SP. Reverse Transcriptase and the Generation of Retroviral DNA. In: Coffin, JM.; Hughes, SH.; Varmus, HE., editors. Retroviruses. Cold Spring Harbor Laboratory Press; Cold Spring Harbor: 1997. p. 121-160.
2. Marquet R, Isel C, Ehresmann C, Ehresmann B. tRNAs as primer of reverse transcriptases. Biochimie. 1995; 77:113–24. [PubMed: 7541250]
3. Cobrinik D, Soskey L, Leis J. A retroviral RNA secondary structure required for efficient initiation of reverse transcription. JVirol. 1988; 62:3622–30. [PubMed: 2458484]
4. Cordell B, Swanstrom R, Goodman HM, Bishop JM. tRNATrp as primer for RNA-directed DNA polymerase: structural determinants of function. J Biol Chem. 1979; 254:1866–74. [PubMed: 84811]
5. Harrich D, Hooker B. Mechanistic aspects of HIV-1 reverse transcription initiation. Rev Med Virol. 2002; 12:31–45. [PubMed: 11787082]
6. Gotte M, Li X, Wainberg MA. HIV-1 reverse transcription: a brief overview focused on structure-function relationships among molecules involved in initiation of the reaction. Arch Biochem Biophys. 1999; 365:199–210. [PubMed: 10328813]

7. Le Grice SF. “In the beginning”: initiation of minus strand DNA synthesis in retroviruses and LTR-containing retrotransposons. Biochemistry. 2003; 42:14349–55. [PubMed: 14661945]
8. Tisne C. Structural bases of the annealing of primer tRNA(3Lys) to the HIV-1 viral RNA. Curr HIV Res. 2005; 3:147–56. [PubMed: 15853720]
9. Abbink TE, Berkhout B. HIV-1 reverse transcription initiation: a potential target for novel antivirals? Virus Res. 2008; 134:4–18. [PubMed: 18255184]
10. Isel C, Ehresmann C, Marquet R. Initiation of HIV reverse transcription. Viruses. 2010; 2:213–243. [PubMed: 21994608]
11. Isel C, et al. Specific initiation and switch to elongation of human immunodeficiency virus type 1 reverse transcription require the post-transcriptional modifications of primer tRNA3Lys. EMBO J. 1996; 15:917–24. [PubMed: 8631312]
12. Lanchy JM, Ehresmann C, Le Grice SF, Ehresmann B, Marquet R. Binding and kinetic properties of HIV-1 reverse transcriptase markedly differ during initiation and elongation of reverse transcription. Embo J. 1996; 15:7178–87. [PubMed: 9003793]
13. Lanchy JM, et al. Contacts between reverse transcriptase and the primer strand govern the transition from initiation to elongation of HIV-1 reverse transcription. J Biol Chem. 1998; 273:24425–32. [PubMed: 9733733]
14. Goldschmidt V, et al. Structural variability of the initiation complex of HIV-1 reverse transcription. J Biol Chem. 2004; 279:35923–31. [PubMed: 15194685]
15. Wilkinson KA, et al. High-throughput SHAPE analysis reveals structures in HIV-1 genomic RNA strongly conserved across distinct biological states. PLoS Biol. 2008; 6:e96. [PubMed: 18447581]
16. Liang C, et al. Mechanistic studies of early pausing events during initiation of HIV-1 reverse transcription. J Biol Chem. 1998; 273:21309–15. [PubMed: 9694891]
17. Thrall SH, et al. Pre-steady-state kinetic characterization of RNA-primed initiation of transcription by HIV-1 reverse transcriptase and analysis of the transition to a processive DNA-primed polymerization mode. Biochemistry. 1998; 37:13349–58. [PubMed: 9786651]
18. Lanchy JM, et al. Dynamics of the HIV-1 reverse transcription complex during initiation of DNA synthesis. J Biol Chem. 2000; 275:12306–12. [PubMed: 10766870]
19. Rong L, et al. HIV-1 nucleocapsid protein and the secondary structure of the binary complex formed between tRNA(Lys.3) and viral RNA template play different roles during initiation of (−) strand DNA reverse transcription. J Biol Chem. 2001; 276:47725–32. [PubMed: 11602578]
20. Abbondanzieri EA, et al. Dynamic binding orientations direct activity of HIV reverse transcriptase. Nature. 2008; 453:184–9. [PubMed: 18464735]
21. Liu S, Abbondanzieri EA, Rausch JW, Le Grice SF, Zhuang X. Slide into action: dynamic shuttling of HIV reverse transcriptase on nucleic acid substrates. Science. 2008; 322:1092–7. [PubMed: 19008444]
22. DeStefano JJ, Mallaber LM, Fay PJ, Bambara RA. Determinants of the RNase H cleavage specificity of human immunodeficiency virus reverse transcriptase. Nucleic Acids Res. 1993; 21:4330–8. [PubMed: 7692401]
23. Stryer L, Haugland RP. Energy transfer: a spectroscopic ruler. Proc Natl Acad Sci U S A. 1967; 58:719–26. [PubMed: 5233469]
24. Ha T, et al. Probing the interaction between two single molecules: fluorescence resonance energy transfer between a single donor and a single acceptor. Proc Natl Acad Sci U S A. 1996; 93:6264–8. [PubMed: 8692803]
25. Iwatani Y, Rosen AE, Guo J, Musier-Forsyth K, Levin JG. Efficient initiation of HIV-1 reverse transcription in vitro. Requirement for RNA sequences downstream of the primer binding site abrogated by nucleocapsid protein-dependent primer-template interactions. J Biol Chem. 2003; 278:14185–95. [PubMed: 12560327]
26. Huang H, Chopra R, Verdine GL, Harrison SC. Structure of a covalently trapped catalytic complex of HIV-1 reverse transcriptase: implications for drug resistance. Science. 1998; 282:1669–75. [PubMed: 9831551]
27. Sarafianos SG, et al. Crystal structure of HIV-1 reverse transcriptase in complex with a polypurine tract RNA:DNA. Embo J. 2001; 20:1449–61. [PubMed: 11250910]

28. Isel C, et al. Structural basis for the specificity of the initiation of HIV-1 reverse transcription. Embo J. 1999; 18:1038–48. [PubMed: 10022845]
29. Paillart JC, et al. First snapshots of the HIV-1 RNA structure in infected cells and in virions. J Biol Chem. 2004; 279:48397–403. [PubMed: 15355993]
30. Suo Z, Johnson KA. Effect of RNA secondary structure on the kinetics of DNA synthesis catalyzed by HIV-1 reverse transcriptase. Biochemistry. 1997; 36:12459–67. [PubMed: 9376350]
31. Thomas JA, Gorelick RJ. Nucleocapsid protein function in early infection processes. Virus Res. 2008; 134:39–63. [PubMed: 18279991]
32. Rein A, Henderson LE, Levin JG. Nucleic-acid-chaperon activity of retroviral nucleocapsid proteins: significance for viral replication. TrendsBiochem Sci. 1998; 23:297–301.
33. Herschlag D. RNA chaperones and the RNA folding problem. J Biol Chem. 1995; 270:20871–20874. [PubMed: 7545662]
34. Rodriguez-Rodriguez L, Tsuchihashi Z, Fuentes GM, Bambara RA, Fay PJ. Influence of human immunodeficiency virus nucleocapsid protein on synthesis and strand transfer by the reverse transcriptase in vitro. J Biol Chem. 1995; 270:15005–11. [PubMed: 7541033]
35. Wu W, et al. Human immunodeficiency virus type 1 nucleocapsid protein reduces reverse transcriptase pausing at a secondary structure near the murine leukemia virus polypurine tract. J Virol. 1996; 70:7132–7142. [PubMed: 8794360]
36. Ji X, Klarmann GJ, Preston BD. Effect of human immunodeficiency virus type 1 (HIV-1) nucleocapsid protein on HIV-1 reverse transcriptase activity in vitro. Biochemistry. 1996; 35:132–143. [PubMed: 8555166]
37. Grohmann D, Godet J, Mely Y, Darlix JL, Restle T. HIV-1 nucleocapsid traps reverse transcriptase on nucleic acid substrates. Biochemistry. 2008; 47:12230–40. [PubMed: 18947237]
38. Tanchou V, Gabus C, Rogemond V, Darlix JL. Formation of stable and functional HIV-1 nucleocapsid complexes in vitro. J Mol Biol. 1995; 252:563–571. [PubMed: 7563074]
39. Lori F, et al. Viral DNA carried by human immunodeficiency virus type 1 virions. J Virol. 1992; 66:5067–74. [PubMed: 1378514]
40. Trono D. Partial reverse transcripts in virions from human immunodeficiency and murine leukemia viruses. J Virol. 1992; 66:4893–900. [PubMed: 1378513]
41. Zhang H, Dornadula G, Orenstein J, Pomerantz RJ. Morphologic changes in human immunodeficiency virus type 1 virions secondary tointravirion reverse transcription: evidence indicating that reverse transcription may not take place within the intact viral core. J Hum Virol. 2000; 3:165–72. [PubMed: 10881997]
42. Houzet L, et al. Nucleocapsid mutations turn HIV-1 into a DNA-containing virus. Nucleic Acids Res. 2008; 36:2311–9. [PubMed: 18296486]
43. Thomas JA, Bosche WJ, Shatzer TL, Johnson DG, Gorelick RJ. Mutations in human immunodeficiency virus type 1 nucleocapsid protein zinc fingers cause premature reverse transcription. J Virol. 2008; 82:9318–28. [PubMed: 18667500]
44. Beerens N, Groot F, Berkhout B. Initiation of HIV-1 reverse transcription is regulated by a primer activation signal. J Biol Chem. 2001; 276:31247–56. [PubMed: 11384976]
45. Wu T, et al. Fundamental differences between the nucleic acid chaperone activities of HIV-1 nucleocapsid protein and Gag or Gag-derived proteins: Biological implications. Virology. 2010; 405:556–567. [PubMed: 20655566]
46. Hooker CW, Lott WB, Harrich D. Inhibitors of human immunodeficiency virus type 1 reverse transcriptase target distinct phases of early reverse transcription. J Virol. 2001; 75:3095–104. [PubMed: 11238836]
47. Rigourd M, et al. Inhibition of the initiation of HIV-1 reverse transcription by 3′-azido-3′-deoxythymidine. Comparison with elongation. J Biol Chem. 2000; 275:26944–51. [PubMed: 10864929]
48. Le Grice SFJ, Cameron CE, Benkovic SJ. Purification and characterization of human immunodeficiency virus type 1 reverse transcriptase. Methods Enzymol. 1995; 262:130–147. [PubMed: 8594344]

49. Rausch JW, Sathyanarayana BK, Bona MK, Le Grice SF. Probing contacts between the ribonuclease H domain of HIV-1 reverse transcriptase and nucleic acid by site-specific photocross-linking. J Biol Chem. 2000; 275:16015–22. [PubMed: 10748161]
50. Lapham J, Crothers DM. RNase H cleavage for processing of in vitro transcribed RNA for NMR studies and RNA ligation. RNA. 1996; 2:289–296. [PubMed: 8608452]
51. Rasnik I, McKinney SA, Ha T. Nonblinking and long-lasting single-molecule fluorescence imaging. Nat Methods. 2006; 3:891–893. [PubMed: 17013382]
52. Venezia CF, Howard KJ, Ignatov ME, Holladay LA, Barkley MD. Effects of efavirenz binding on the subunit equilibria of HIV-1 reverse transcriptase. Biochemistry. 2006; 45:2779–89. [PubMed: 16503633]
53. Kapanidis AN, et al. Fluorescence-aided molecule sorting: analysis of structure and interactions by alternating-laser excitation of single molecules. Proc Natl Acad Sci U S A. 2004; 101:8936–8941. [PubMed: 15175430]
54. Thompson RE, Larson DR, Webb WW. Precise Nanometer Localization Analysis for Individual Fluorescent Probes. Biophys J. 2002; 82:2775–2783. [PubMed: 11964263]
55. Yildiz A, et al. Myosin V walks hand-over-hand single fluorophore imaging with 1.5-nm localization. Science. 2003; 300:2061–2065. [PubMed: 12791999]

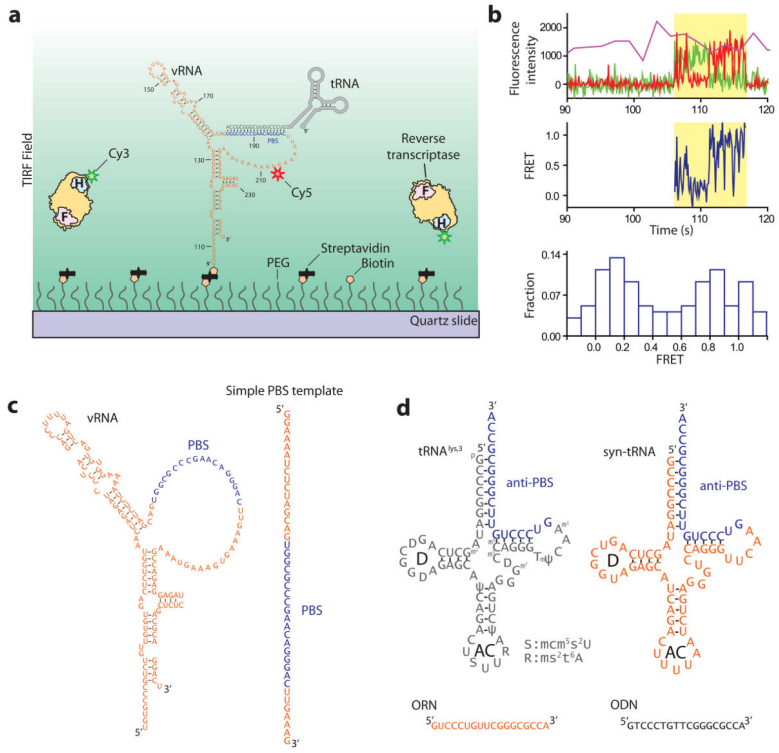

Figure 1.

Single-molecule FRET assay for probing the structural dynamics of the initiation complex. (**a**) The vRNA template (orange) is labeled with a FRET acceptor (Cy5, red star) near the PBS (blue), annealed to a tRNA primer (grey), and immobilized to the PEG-coated surface via a streptavidin-biotin linkage. The surface-anchored tRNA:vRNA substrates are immersed in a solution containing RT (yellow) labeled with the FRET donor (Cy3, green star). The fingers and RNase H domains of RT are indicated by F and H, respectively. Fluorescence signal from single tRNA:vRNA:RT complexes are detected using a TIRF microscope. (**b**) FRET analysis of RT binding events. The upper panel shows the fluorescence signals from Cy3 (green) and Cy5 (red) under 532 nm illumination and the signal from Cy5 directly excited by 635 nm illumination (purple). Binding of RT to the substrate (highlighted by yellow) results in an increase in the total fluorescence signals from Cy3 and Cy5 under 532 nm illumination due to excitation of the FRET donor, but does not affect the Cy5 signal from direct excitation by 635 nm light. (Middle panel) FRET values during the binding event. (Lower panel) FRET histogram of the binding event. (**c**) Sequences of the vRNA and simple RNA PBS templates studied in this work. (**d**) Sequences of the natural $tRNA^{Lys,3}$, synthetic tRNA (syn-tRNA), oligoribonucleotide (ORN) and oligodeoxyribonucleotide (ODN) primers.

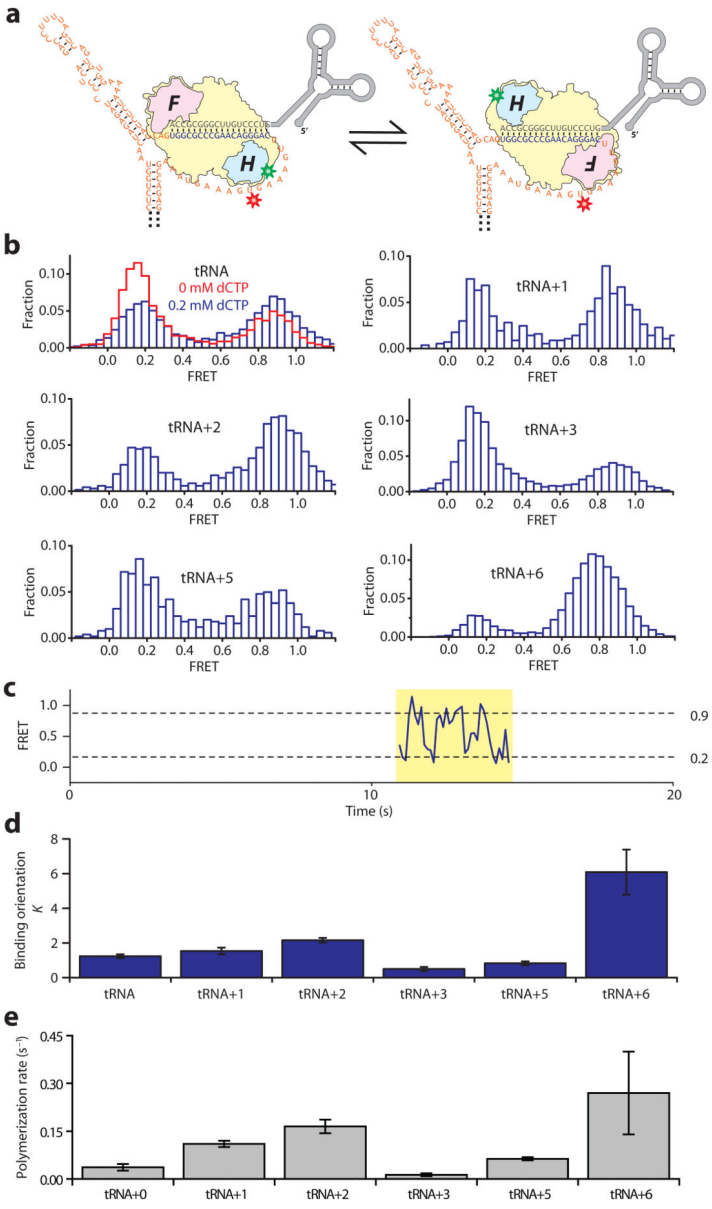

Figure 2.

RNA-dependent DNA polymerase activity of RT correlates with its binding orientation in the initiation complex. (**a**) A cartoon illustrating RT bound to the tRNA:vRNA complex in the polymerase-competent (left) and flipped (right) orientations. (**b**) The FRET distribution obtained when Cy3-labeled RT binds to Cy5-labeled tRNA+*n*:vRNA complexes in the presence of 200 μM cognate dNTP. In the case of tRNA (*n* = 0), the FRET distribution in the absence of dNTP (red) is also shown. The FRET distributions for other *n* values in the absence of dNTP are shown in Supplementary Fig. 5. (**c**) A representative time trace of an RT binding event (highlighted in yellow) shows spontaneous transitions between the high and low FRET states. (**d**) The equilibrium constants *K* between the polymerase-competent and the flipped binding orientations of RT in the presence of 200 μM cognate dNTP. Error bars are s.e.m. from at least 3 independent experiments. (**e**) Primer extension rates on the

vRNA template. The primer extension rate is highly correlated with the binding orientation equilibrium *K*, exhibiting a correlation coefficient of 0.94. Error bars are s.d. from at least 3 independent experiments.

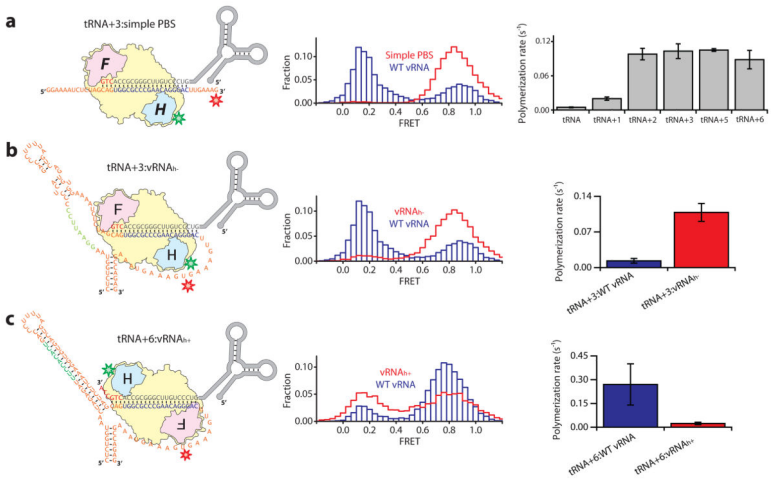

Figure 3.

The stem-loop structure upstream of the PBS causes the major pauses during initiation and governs the initiation-to-elongation transition. (**a**) Left panel: Cartoon of RT bound to tRNA +3:simple PBS substrate. Middle Panel: FRET histograms for RT bound to tRNA+3 primers annealed to the vRNA template (blue) and simple PBS template (red). Right panel: Rates of single nucleotide addition to various tRNA primers on the simple PBS template. (**b**) Left panel: Cartoon of RT bound to tRNA+3: $vRNA_{h-}$ substrate. Middle Panel: FRET histograms for RT bound to tRNA+3 primers annealed to wild type (WT) vRNA (blue) and $vRNA_{h-}$ (red) templates. Right panel: Rates of single nucleotide addition to tRNA+3 primers annealed to WT vRNA (blue) and $vRNA_{h-}$ (red) templates. (**c**) Left panel: Cartoon of RT bound to tRNA+6: $vRNA_{h+}$ substrate. Middle Panel: FRET histograms for RT bound to tRNA+6 primers annealed to WT vRNA (blue) and $vRNA_{h+}$ (red) templates. Right panel: Rates of single nucleotide addition to tRNA+6 primers annealed to WT vRNA (blue) and $vRNA_{h+}$ (red) templates. The nucleotides mutated to create the $vRNA_{h-}$ and $vRNA_{h+}$ constructs are shown in green. Error bars are s.d. from at least 3 independent experiments.

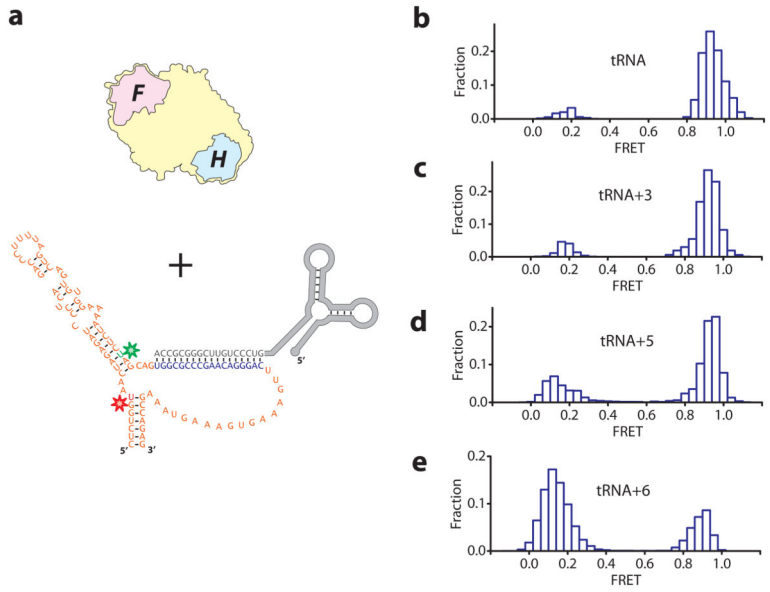

Figure 4.

Disruption of the stem-loop structure upstream of the PBS occurs upon addition of the 6th nucleotide to the tRNA primer. (**a**) Diagram of the doubly-labeled construct used to monitor the folding of the stem-loop structure. Cy3 (green star) and Cy5 (red star) are attached to vRNA positions U132 and U177. (**b–e**) The FRET distributions obtained when 100 nM RT was added to the doubly-labeled template annealed to the tRNA (**b**), tRNA+3 (**c**), tRNA+5 (**d**), and tRNA+6 (**e**) primers.

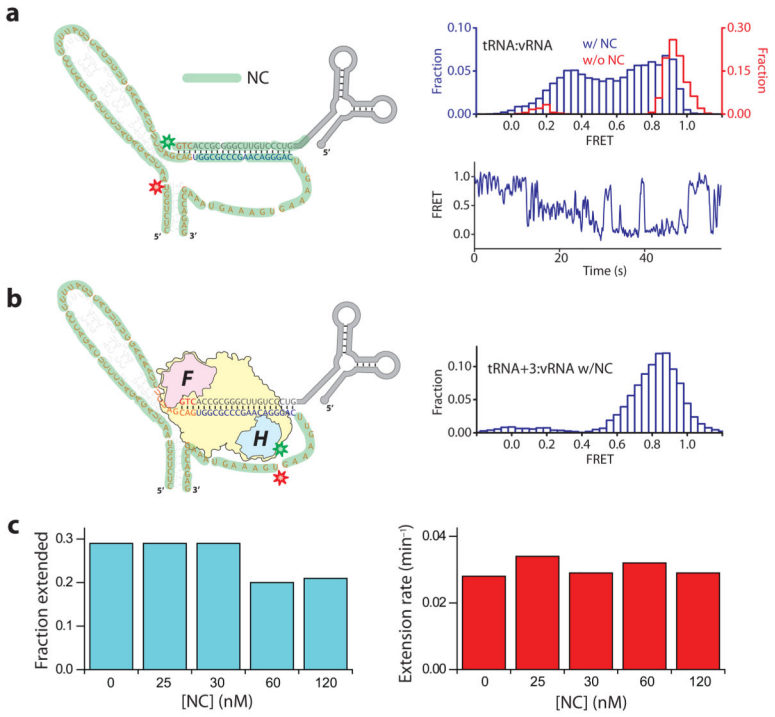

Figure 5.

HIV-1 NC destabilizes the stem-loop structure. (**a**) Left: Cartoon of the doubly-labeled tRNA:vRNA construct complexed with NC (green). Upper right: FRET distributions obtained from the doubly labeled tRNA:vRNA substrate in the absence (red) or presence (blue) of 1 μM NC. Lower right: a representative FRET time trace in the presence of 1 μM NC. (**b**) FRET distribution obtained for Cy3-labeled RT bound to Cy5-labeled vRNA:tRNA +3 complexes in the presence of 10 nM NC. (**c**) Single-nucleotide extension kinetics of tRNA+3:vRNA complex in the presence of 20 nM RT and various concentrations of NC. Left: The fraction of tRNA primers extended by a single nucleotide. Right: Primer extension rate constants.

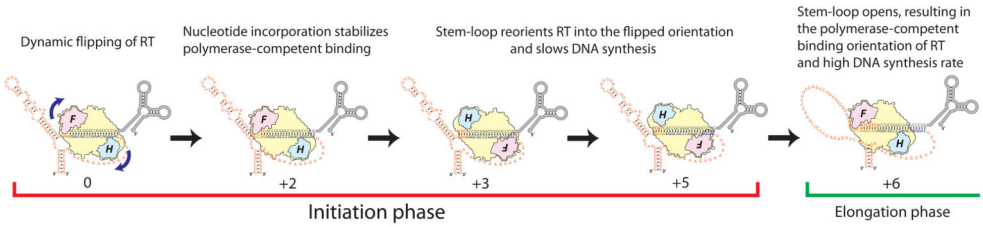

Figure 6.

Structural dynamics of the HIV-1 initiation complex regulate the early phases of reverse transcription. RT binds to the initiation complex in two orientations — a polymerase-competent orientation and a flipped, polymerase-inactive orientation. RT spends a large portion of time bound to the tRNA:vRNA substrate in the flipped orientation. Addition of the first couple of deoxyribonucleotides to the tRNA primer shifts the RT binding equilibrium towards the polymerase-competent orientation and increases the DNA synthesis rate. The synthesis rate drops dramatically at position +3, where RT encounters a stem-loop structure in the vRNA template that forces the enzyme to bind predominantly in the flipped orientation, thereby increasing the probability of pausing. Strand-displacement synthesis until the +6 position eventually leads to unfolding of the stem-loop, which allows RT to reorient into the polymerase-competent binding mode and enter the fast, processive elongation phase of DNA synthesis.